Progress In Electromagnetics Research B, Vol. 52, 185–205, 2013

DECOMPOSITION-BASED EVOLUTIONARY MULTI-OBJECTIVE OPTIMIZATION APPROACH TO THE DESIGN OF CONCENTRIC CIRCULAR ANTENNA ARRAYS

Subhodip Biswas[1], Digbalay Bose[1], Swagatam Das[2, *], and Souvik Kundu[1]

[1]Department of Electronics and Telecommunication Engineering, Jadavpur University, Kolkata 700 032, India

[2]Electronics and Communication Sciences Unit, Indian Statistical Institute, Kolkata 700 108, India

Abstract—We investigate the design of Concentric Circular Antenna Arrays (CCAAs) with $\lambda/2$ uniform inter-element spacing, non-uniform radial separation, and non-uniform excitation across different rings, from the perspective of Multi-objective Optimization (MO). Unlike the existing single-objective design approaches that try to minimize a weighted sum of the design objectives like Side Lobe Level (SLL) and principal lobe Beam-Width (BW), we treat these two objectives individually and use Multiobjective Evolutionary Algorithm based on Decomposition (MOEA/D) with Differential Evolution (DE), called MOEA/D-DE, to achieve the best tradeoff between the two objectives. Unlike the single-objective approaches, the MO approach provides greater flexibility in the design by yielding a set of equivalent final (non-dominated) solutions, from which the user can choose one that attains a suitable trade-off margin as per requirements. We illustrate that the best compromise solution attained by MOEA/D-DE can comfortably outperform state-of-the-art variants of single-objective algorithms like Particle Swarm Optimization (PSO) and Differential Evolution. In addition, we compared the results obtained by MOEA/D-DE with those obtained by one of the most widely used MO algorithm called NSGA-2 and a multi-objective DE variant, on the basis of the R-indicator, hypervolume indicator, and quality of the best trade-off solutions obtained. Our simulation results clearly indicate the superiority of the design based on MOEA/D-DE.

Received 7 March 2013, Accepted 31 May 2013, Scheduled 4 June 2013

* Corresponding author: Swagatam Das (swagatamdas19@yahoo.co.in).

1. INTRODUCTION

Circular or ring-shaped arrays consist of a number of radiating elements arranged on a circle. They offer the advantage of an all-azimuth scan capability along with the invariance of the beam-pattern [1–3]. If several circular arrays with different radii share the same center then the resulting planar array is a Concentric Circular Antenna Array (CCAA). CCAAs offer several advantages over other array configurations including the flexibility in array pattern synthesis and design both in narrowband and broadband beamforming applications [3–7].

CCAAs provide nearly invariant azimuth angle coverage for Direction of Arrival (DOA) applications [8, 9]. Recently there has been a surge of interest in the design of CCAAs with the derivative-free nature-inspired metaheuristics like Particle Swarm Optimization (PSO) [10]. Mandal et al. [11] applied a Craziness-based PSO (CRPSO) and CRPSO with Wavelet Mutation (CRPSOWM) to the process of optimal designing three-ring concentric circular antenna arrays (CCAAs) focused on Sidelobe Level (SLL) reduction. Mandal et al. [12] investigated the SLL reductions without and with central element feeding in various designs of three-ring concentric circular antenna arrays (CCAA) using PSO with Constriction Factor Approach (PSOCFA). Pathak et al. [13] employed a modified PSO algorithm for thinning large multiple concentric circular ring arrays of uniformly excited isotropic antennas to generate a pencil beam in the vertical plane with minimum relative side lobe level.

Existing approaches, such as [11, 12], combine separate objectives (which are often conflicting) through a weighted linear sum into a single aggregated objective function. The weighted sum method is, however, very often subjective, and the solution is sensitive to the values (more precisely, the relative values) of the weights specified. It is hard, if not impossible, to find a universal set of weights, that click on different instantiations of the same problem. Motivated by the inherent multi-objective nature of the CCAA design problems and the overwhelming growth in the field of Multi-Objective Evolutionary Algorithms (MOEAs), we started to look for the most recently developed MOEAs that could solve the concentric array synthesis problem much more efficiently as compared to the conventional single-objective approaches. Our search finally converged to a decomposition-based MOEA, called MOEA/D-DE [14, 15], that ranked first among 13 state-of-the-art MOEAs in the unconstrained MOEA competition held under the IEEE Congress on Evolutionary Computation (CEC) 2009 [16]. MOEA/D-DE uses Differential Evolution (DE) [17, 18] as its main search strategy and decomposes an MO problem into a number of scalar optimization sub-problems to optimize them simultaneously. Each sub-problem is optimized by only using information from its several neighboring sub-problems and this feature considerably reduces the computational complexity of the algorithm.

In this paper, we present a multi-objective formulation for the design of ring symmetric excited CCAA with non-uniform radial separation and use MOEA/D-DE to obtain an optimal design. We consider the primary lobe beamwidth and SLL as the two objectives. Thus the primary design variables at our disposal are:

a) Number of elements in the first ring (N_1).
b) Number of rings in the CCAA (M).

The contribution of the present work is two-fold. Firstly, to the best of our knowledge, this is the first work that deals with the design of CCAA as a multi-objective optimization problem and attempts to achieve the best trade-off between two important objectives like BW and SLL. Our approach is of course motivated by the recently reported success of evolutionary multi-objective optimization techniques to the design of linear arrays [19, 20], time-modulated antenna arrays [21], and monopulse arrays [22].

Secondly, we carry out a parametric study to show how the solutions depend on two crucial parameters — N_1 and M. For each pair of N_1 and M we get a set of Pareto optimal solutions that lie on a trade-off curve drawn in the bi-objective function space. We compare the change in the quality of the solutions obtained for varying N_1 and M by tabulating the best compromise solutions. This gives a valuable insight to the antenna designer on how to determine N_1 and M for a particular design requirement. This can be a valuable tool to help determine N_1 and M such that particular design requirements are met. Many works in literature have dealt with optimal design of CCAA but they have not sufficiently dealt with the design aspects of the problem or proposed a way to determine the parameters to help design CCAA.

Since unlike single-objective optimization techniques (that finish with a single best solution) the MOEAs return a set of non-dominated solutions (the Pareto optimal set, to be briefly outlined in Section 2), we used a fuzzy membership function based approach [23, 24] to identify the best compromise solutions over each case. To evaluate the performance of the proposed design method, we compare the best trade-off solutions returned by MOEA/D-DE with those obtained with state-of-the-art single-objective algorithms like CLPSO (Comprehensive Learning based PSO) [25], DEGL (DE with Global and Local Neighborhoods) [26] and also with the performance of an UCCAA designed following the method of Dessouky et al. [7]. The results of MOEA/D-DE are also compared with those of two other well-known multi-objective algorithms like Non-Dominated Sorting Genetic Algorithm (NSGA-II) [27] and Multi-Objective DE (MODE) [28] that optimize the same two design objectives, on the basis of the hypervolume indicator and the R-indicator (I_{R2}) [29] metrics. Our simulation experiments indicate the superiority of the multi-objective optimization methodology over the conventional approaches to the design of CCAAs.

2. THE MOEA/D-DE ALGORITHM — AN OUTLINE

Due to the multiple criteria-based nature of most real-world problems, Multi-objective Optimization (MO) problems are ubiquitous, particularly throughout engineering applications. As the name indicates, multi-objective optimization problems involve multiple objectives, which should be optimized simultaneously and that often are in conflict with each other. This results in a group of alternative solutions which must be considered equivalent in the absence of information concerning the relevance of the others. The concepts of *dominance* and *Pareto-optimality* may be presented more formally in the following way [30, 31].

2.1. General MO Problems

Definition 1: Consider without loss of generality the following multi-objective optimization problem with D decision variables x (parameters) and n objectives y:

$$\text{Minimize: } \vec{Y} = f\left(\vec{X}\right) = \left(f_1(x_1, \ldots, x_D), \ldots, f_n\left(x_1, \ldots, x_D\right)\right) \quad (1)$$

where $\vec{X} = [x_1, \ldots, x_D]^T \in P$ and $\vec{Y} = [y_1, \ldots, y_n]^T \in O$ and $\vec{X}$ is called decision (parameter) vector, P is the parameter space, $\vec{Y}$ is the objective vector, and O is the objective space. A decision vector $\vec{A} \in P$ is said to dominate another decision vector $\vec{B} \in P$ (also written as $\vec{A} \prec \vec{B}$ for minimization) if and only if:

$$\forall i \in \{1, \ldots, n\}: \; f_i\left(\vec{A}\right) \leq f_i\left(\vec{B}\right) \quad \wedge \exists j \in \{1, \ldots, n\}: \; f_j\left(\vec{A}\right) < f_j\left(\vec{B}\right) \quad (2)$$

Based on this convention, we can define non-dominated, *Pareto-optimal* solutions as follows:

Definition 2: Let $\vec{A} \in P$ be an arbitrary decision vector.

(a) The decision vector $\vec{A}$ *is said to be* non-dominated regarding the set $P' \subseteq P$ if and only if there is no vector in P' which can dominate $\vec{A}$.

(b) The decision (parameter) vector $\vec{A}$ is called Pareto-optimal if and only if $\vec{A}$ is non-dominated regarding the whole parameter space P.

2.2. The MOEA/D-DE Algorithm

Multi-objective evolutionary algorithm based on decomposition was first introduced by Zhang and Li in 2007 [32] and extended with DE-based reproduction operators in [14, 15]. Instead of using non-domination sorting for different objectives, the MOEA/D algorithm decomposes a multi-objective optimization problem into a number of single objective optimization sub-problems by using weights vectors λ and optimizes them simultaneously. Each sub-problem is optimized by sharing information between its neighboring sub-problems with similar weight values. MOEA/D uses Tchebycheff decomposition approach [33] to convert the problem of approximating the PF into a number of scalar optimization problems. Let $\vec{\lambda}^1, \ldots, \vec{\lambda}^{Np}$ be a set of evenly spread weight vectors and $\vec{Y}^* = (y_1^*, y_2^*, \ldots, y_M^*)$ be a reference point, i.e., for minimization problem, $y_i^* = \min\{f_i(\vec{X})|\vec{X} \in \Omega\}$ for each $i = 1, 2, \ldots, M$. Then the problem of approximation of the PF can be decomposed into Nscalar optimization subproblems by Tchebycheff approach and the objective function of the j-th subproblem is:

$$g^{te}\left(\vec{X}|\vec{\lambda}^j, \vec{Y}^*\right) = \max_{1\leq i\leq M}\left\{\lambda_i^j \left|f_i(x) - y_i^*\right|\right\}, \tag{3}$$

where $\vec{\lambda}^j = (\lambda_1^j, \ldots, \lambda_M^j)^T$, $j = 1, \ldots, Np$ is a weight vector, i.e., $\lambda_i^j \geq 0$ for all $i = 1, 2, \ldots, m$ and $\sum\limits_{i=1}^{m} \lambda_i^j = 1$. MOEA/D minimizes all these N objective functions simultaneously in a single run. Neighborhood relations among these single objective subproblems are defined based on the distances among their weight vectors. Each subproblem is then optimized by using information mainly from its neighboring subproblems. In MOEA/D, the concept of neighborhood, based on similarity between weight vectors with respect to Euclidean distances, is used to update the solution. The neighborhood of the i-th subproblem consists of all the subproblems with the weight vectors from the neighborhood of $\vec{\lambda}^i$. At each generation, the MOEA/D maintains following variables:

1. A population A population $\vec{X}_i, \ldots, \vec{X}_{N_p}$ with size Np, where $\vec{X}_i$ is the current solution to the i-th subproblem.
2. The fitness values of each population corresponding to a specific subproblem.

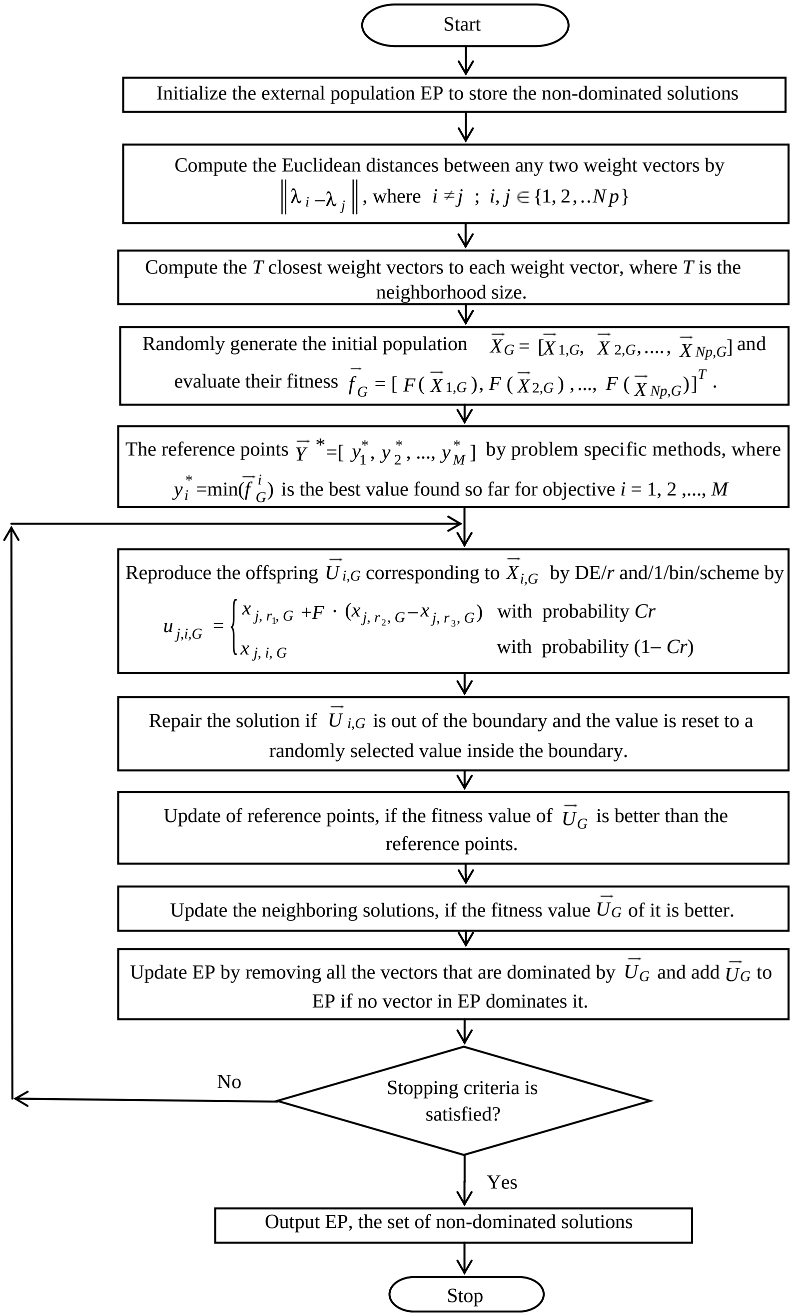

Figure 1. Flowchart of MOEA/D-DE algorithm.

3. The reference point $\vec{Y}^* = (y_1^*, y_2^*, \dots, y_M^*)$, where y_i^* is the best value found so far for objective i.
4. An external population (EP), which is used to store non-dominated solutions found during the search.

The flowchart of the MOEA/D-DE algorithm is presented in Figure 1.

For MOEA/D-DE, the best compromise solution was chosen from the PF using the method described in [23, 24]. The ith objective function f_i is represented by a membership function μ_i defined as:

$$\mu_i = \left\{ \begin{array}{ll} 1, & f_i \le f_i^{\min} \\ \frac{f_i^{\max} - f_i}{f_i^{\max} - f_i^{\min}}, & f_i^{\min} < f_i < f_i^{\max} \\ 0, & f_i \ge f_i^{\max} \end{array} \right\} \tag{4}$$

where $f_i^{\min}$ and $f_i^{\max}$ are the minimum and maximum value of the ith objective solution among all non-dominated solutions, respectively. For each non-dominated solution q, the normalized membership function μ^q is calculated as:

$$\mu^q = \frac{\sum\limits_{i=1}^{N_{obj}} \mu_i^q}{\sum\limits_{k=1}^{N_s} \sum\limits_{i=1}^{N_{obj}} \mu_i^k}, \tag{5}$$

where N_s is the number of non-dominated solution. The best compromise is the one having the maximum value of μ^q.

A detailed flowchart illustrating the dynamics of the MOEA/D-DE is given in Figure 1.

3. MULTI-OBJECTIVE FORMULATION OF CCAA DESIGN PROBLEM

CCAA consists of antenna elements arranged in multiple concentric circular rings which differ in radius and number of elements. This leads to different radiation patterns for different configurations and parameters of CCAA.

Figure 2 shows the configuration of multiple concentric circular arrays in XY plane which consists of M concentric circular rings. The mth ring has a radius r_m and N_m number of isotropic elements where $m = 1, 2, \dots, M$. Since here we are considering a CCAA where the elements are considered to be equally spaced along a common circle. The far field pattern in free space is given by:

$$E(\theta, \phi) = 1 + \sum_{m=1}^{M} \sum_{n=1}^{N_m} I_m \cdot \exp\left(jkr_m \sin\theta \cos(\phi - \phi_{mn})\right) \tag{6}$$

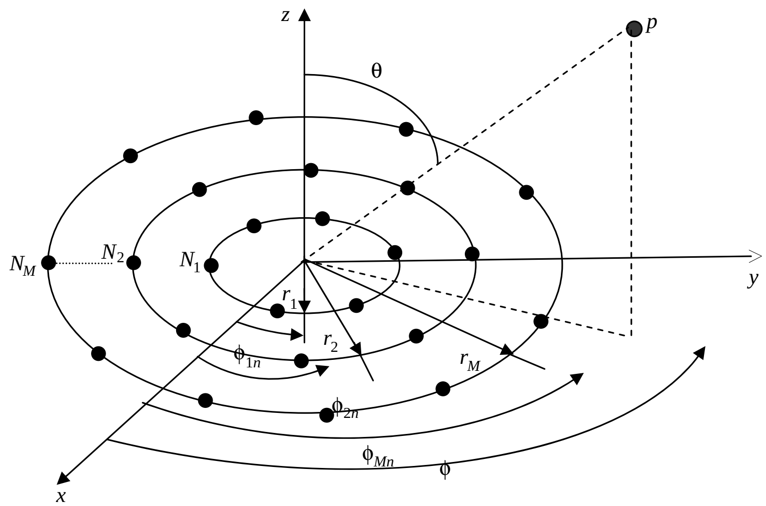

Figure 2. Concentric circular antenna array (CCAA).

Normalized power pattern $P(\theta, \phi)$ in dB can be expressed as:

$$P(\theta, \phi) = 10 \log_{10} \left[\frac{|E(\theta, \phi)|}{|E(\theta, \phi)|_{\max}} \right]^2 \tag{7}$$

where,

r_m = radius of mth ring = $N_m d_m / 2\pi$.

d_m = inter-element arc spacing of mth circle

$\phi_{mn} = 2\pi n / N_m$ = angular position of nth element of mth ring.

ϕ = azimuth angle, k = wave number = $2\pi/\lambda$.

I_m = excitation amplitude of the elements in mth ring. In this design all the elements in a particular ring are given the same excitation.

For non-uniform radial separation [37],

$$r_{m+1} = r_m + \frac{\lambda}{2} + \Delta_m \lambda, \quad \text{where } 0 \leq \Delta_m \leq 1. \tag{8}$$

However we desire to keep the inter-element spacing at $\lambda/2$. The number of equally spaced elements in mth ring is:

$$N_m = \frac{2\pi r_m}{\lambda/2}. \tag{9}$$

The number of elements in the first ring needs to be fixed by the antenna designer. Simultaneously r_1 can be determined. The two objectives are primary lobe BW and SLL. Next we provide a mathematical formulation for the two objectives.

The far field pattern $E(\theta, \phi)$ can actually be considered as a function of θ only because it is symmetrical with respect to ϕ. Hence for further analysis we will consider $E(\theta)$. The SLL is taken as the decibel level of the sidelobe. To calculate the sidelobe level we calculate where the array factor reaches local maxima, and the maximum value of all the local maxima gives us the SLL value.

Let $\zeta = \{\theta \in \psi | E(\theta) > E(\theta - \Delta\theta) \Lambda E(\theta) > E(\theta + \Delta\theta) \Lambda \theta \neq 0°\}$ be the set of angles where local maxima of $E(\theta)$ occur. We exclude $\theta = 0°$ because at this angle we have the maximum radiation due to the principal lobe. Also Let $\Phi = \{\theta \in \psi | E(\theta) < E(\theta - \Delta\theta) \Lambda E(\theta) < E(\theta + \Delta\theta)\}$ be the set of angles where local minima of $E(\theta)$ is reached. Let the local minimum closest to 0° be α. Therefore $\alpha = \min(\Phi)$. Because of the symmetric property of array pattern the primary lobe beamwidth is 2α.

Now we are at a position to define the two objective functions.

$$f_1 = \max \left[10 \log_{10} \left(\frac{E(\zeta)}{E(0°)} \right)^2 \right] \tag{10a}$$

$$f_2 = 2 \cdot \min(\Phi) . \tag{10b}$$

Both the objectives need to be minimized. However the dynamic-range ratio of the source excitation is needed to be a minimum [34]. We impose a constraint on dynamic range ratio in the following form:

$$I_{\max}/I_{\min} \leq 4 \tag{11}$$

The antenna designer can change the constraint according to his own choice. Future research can also be based on minimizing dynamic-range ratio as a separate objective as well. In this paper we deal with CCAAs with non-uniform radial spacing and non-uniform excitation across different rings. Thus we have the control over the excitation amplitudes I_m and additional radial separation Δ_m. Thus, while optimizing I_m we restrict the normalized excitation amplitudes to be in the range (1, 0.25), so that the dynamic range ratio is at most 4 and the constraint is automatically maintained.

4. STUDY OF TRADE-OFF CURVES FOR CCAA DESIGN

The general well accepted figures of merit of an array pattern are primary lobe BW and SLL. We want an array pattern to have thin primary lobe and extremely low sidelobes compared to the primary lobe. In other words we need to minimize both the objective functions for BW and SLL. In this section we investigate how the figures of merit of the array pattern designed depend on the parameters of the CCAA. To study how exactly the array pattern varies with the number of rings (M) and number of elements in the 1st ring (N_1) we will consider two cases. In the first case we will keep N_1 constant and increase the number of rings and detect the best compromise solutions obtained with MOEA/D-DE. In the second case we keep the number of rings constant and investigate the nature of the trade-off curves (best approximated PFs) for different values N_1. Next we keep N_1 constant at a certain value and study the trade-off curves for different number of rings. The control parameters for MOEA/D-DE are set in accordance with [15] and the setup is summarized in Table 3. In what follows we report the best results obtained from a set of 50 independent runs of the algorithm, where each run was continued up to 3×10^5 Function Evaluations (FEs). This is maintained also for the other algorithms in Section 5.

4.1. Case 1: Number of Rings is Constant

Here we fix the number of rings $M = 3$ and show the resulting trade-off curves obtained with MOEA/D-DE for $N_1 = 2, 3, 4, 5, 6, 7$ in Figure 3. In Table 1 we show the best compromise values of the two objectives obtained with MOEA/D-DE for different values of N_1. Table 1 indicates that with increase of N_1, BW decreases. But the SLL does not change uniformly. Thus, there is no significant improvement in the quality of the solution with larger N_1. However greater N_1 does imply greater number of elements in the first ring. Hence a

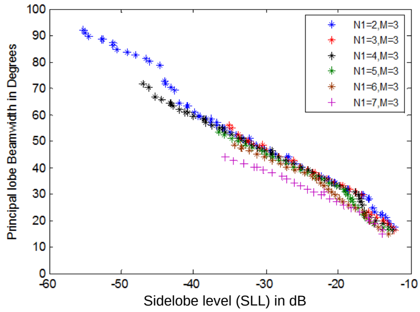

Figure 3. Trade-off curves for Case 1.

N_1	SLL (dB)	BW (degrees)
2	−21.35	34.31
3	−22.13	34.52
4	−22.21	34.13
5	−22.15	33.11
6	−21.76	31.91
7	−22.35	29.50

Table 1. Best compromise table (Case 1).

disadvantage is that with greater number of elements, the design-cost increases.

4.2. Case 2: Number of Elements in 1st Ring Constant

Here we keep N_1 as constant and vary number of rings (M). In other words we take $N_1 = 5$ and show trade-off curves for $M = 3$, 4, 5, 6 and 7 in Figure 4. Table 2 is similar in spirit to Table 1, but this time the best compromise solutions are obtained for varying M. As we increase the number of rings the SLL decreases steadily but there is phenomenal decrease in beamwidth. Thus, we see that to produce narrow beamwidth radiation patterns we need a greater number of rings. Unlike the previous study where we were increasing N_1, increasing M produces radical improvement in the radiation pattern.

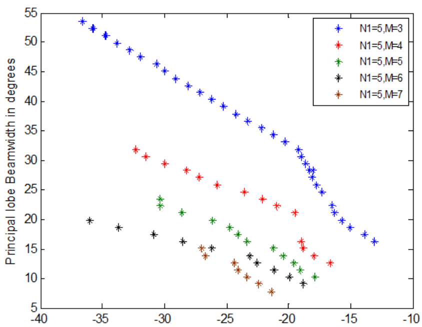

Figure 4. Trade-off curves for Case 2.

M	MSLL (dB)	BW (degrees)
3	−22.15	33.11
4	−23.57	24.68
5	−24.10	17.46
6	−26.18	15.05
7	−26.68	13.85

Table 2. Best compromise table (Case 2).

We see that for $M = 3$, the best compromise solution shows beamwidth equal to 33.11° and for $M = 7$ the best compromise solution has a beamwidth of just 13.85°. Thus, while the beamwidth decreases by 19.26°, the SLL falls only by 4.53 dB. Once again as in the previous study, increasing the number of rings leads to greater number of antenna elements. Hence the antenna designer needs to find a compromise between design cost and quality of radiation pattern.

This parametric study, aided by an MO algorithm, will provide an idea on how to go about deciding the values of N_1 and M so that specific design requirements are met. The designer can perform similar simulations and get approximated PFs for different values of N_1 and M. He can find the approximated PF having a solution closest to the point corresponding to the design requirements. N_1 and M corresponding to that trade-off curve can be taken as the design parameters of the CCAA.

5. COMPARATIVE STUDY WITH OTHER DESIGN METHODS

Over the CCAA design instances, we also compare the performance of MOEA/D-DE with that of two single-objective optimization techniques, namely CLPSO [25] and DEGL [26] that are the state-of-the-art variants of DE and PSO, which have been widely used in past for various electromagnetic optimization tasks, e.g., see [35, 36]. For single-objective optimization techniques, we use a weighted linear sum of the objective functions given in (10a) and (10b). We also compared MOEA/D-DE results with two other MO algorithms: NSGA-2 [28] and MODE [32]. Guidelines for selecting the parameters for all the algorithms are taken from their respective literatures. For MODE, as control parameters we took $F = 0.45$, $Cr = 0.8$, and $NP = 100$. For the NSGA-2 algorithm, we took crossover probability = 0.9, mutation probability = $1/N$ (N being the total number of antenna elements in the array), distribution index for crossover = 20, distribution index for mutation = 20. The detailed parametric setup for MOEA/D-DE and the two single-objective optimization algorithms have been shown in Table 3. For comparing the performance of the MO algorithms, we

Table 3. Parametric set-up for MOEA/D-DE, CLPSO, and DEGL (r_d is the difference between the maximum and minimum values of the d-th decision variable).

MOEA/D-DE		CLPSO		DEGL	
Param.	Val.	Param.	Val.	Param.	Val.
Pop_size	150	Swarm size	150	Pop_size	150
Crossover Probability CR	0.9	C_1	1.494	Crossover Probability CR	0.9
F	0.8	C_2	1.494	F	0.8
distribution index η	20	Inertial Weight w	linearly decreased from 0.9 to 0.2	Neighbor-hood size	15% of Pop_size
mutation rate p_m	$1/N$	$\nu_{d,\max}$	$0.9{*}r_d$	weight factor	fixed, 0.5

used the following performance indices:

(1) R indicator (I_{R2}) [29]: It can be expressed as

$$I_{R2} = \frac{\sum_{\lambda \in \Lambda} u^*(\lambda, A) - u^*(\lambda, R)}{|\Lambda|}, \tag{12}$$

where R is a reference set, u^* is the maximum value reached by the utility function u with weight vector λ on an approximation set A, i.e., $u^* = \max_{y \in A} u_\lambda(y)$. We choose the augmented Tchebycheff function as the utility function.

(2) Hypervolume difference to a reference set ($I_{\bar{H}}$) [29]: The hypervolume indicator I_H measures the hypervolume of the objective space that is weakly dominated by an approximation set A, and is to be maximized. Here we consider the hypervolume difference to a reference set R.

We will refer to this indicator as $I_{\bar{H}}$, which is defined as $I_{\bar{H}} = I_H(R) - I_H(A)$ where smaller values correspond to higher quality as opposed to the original hypervolume I_H.

For comparison purpose, we shall consider the following two cases.

5.1. Case 1: $N_1 = 8$, $M = 4$

The approximated PFs as well as the best compromise solutions obtained by MOEA/D-DE are compared with those achieved with two other MO algorithms — NSGA2 and MODE. The trade-off curves between two design objectives have been shown in Figure 5. The corresponding R-indicator and hypervolume indicator values (best, worst, mean, and standard deviation) are provided in Table 4. These values clearly reveal that the best approximation of the PF

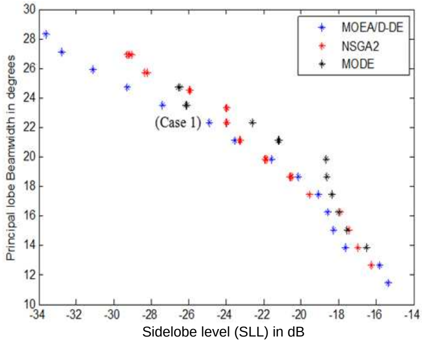

Figure 5. Trade-off curves obtained with three MO algorithms (Case 1).

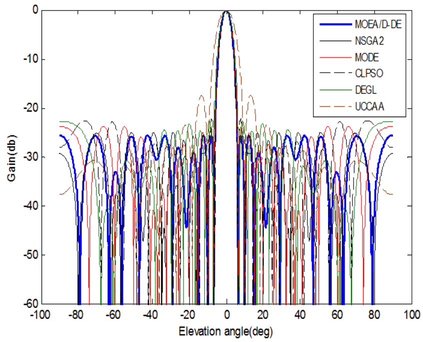

Figure 6. Array pattern for $N_1 = 8$ and $M = 4$.

Table 4. Best, worst, mean, and standard deviations of the performance metrics for comparing the MO algorithms (Case 1).

Performance Metric	Value type	MOEA/D-DE	NSGA-2	MODE
R-indicator	Best	$3.2e-07$	$2.1e-06$	$3.9e-05$
	Worst	$1.9e-05$	$7.7e-04$	$8.3e-04$
	Mean	$4.7e-06$	$8.9e-05$	$1.5e-04$
	Std. Dev.	$6.0e-06$	$3.5e-05$	$1.4e-04$
Hypervolume-indicator	Best	$5.0e-06$	$1.9e-05$	$7.3e-05$
	Worst	$4.5e-05$	$2.1e-03$	$8.2e-03$
	Mean	$9.1e-06$	$7.1e-04$	$2.8e-03$
	Std. Dev.	$2.1e-06$	$7.6e-05$	$6.8e-04$

is obtained for MOEA/D-DE. Array patterns corresponding to the best compromise solution obtained with five algorithms (MOEA/D-DE, NSGA-2, MODE, CLPSO, and DEGL) are shown in Figure 6. The design objective values achieved by these five algorithms are tabulated in Table 5. In Table 5 we also show the design objectives obtained in case of a uniformly spaced and uniformly excited CCAA (marked as UCCAA). Figure 6 and Table 5 clearly indicate that the best array pattern as well as optimal values of the design objectives (for given N_1 and M) can be attained by using MOEA/D-DE.

Table 5. Design objectives achieved.

Objectives	MOEA/D-DE	DEGL	CLPSO	NSGA2	MODE	UCCAA
BW (Degrees)	22.06	22.10	23.38	22.14	22.10	28.83
SLL	−25.31	−20.67	−24.70	−24.05	−22.57	−15.55

5.2. Case 2: $N_1 = 4$, $M = 7$

For this design instance the best approximated PFs generated by three MO algorithms are shown in Figure 7. The corresponding R-indicator and hypervolume indicator values (best, worst, mean, and standard deviation) are provided in Table 6. These values clearly reveal that the best approximation of the PF is obtained for MOEA/D-DE. The array patterns corresponding to the best compromise solution achieved with MOEA/D-DE, MODE, and CLPSO for this case are shown in Figure 8. In the same figure we also provide the array patterns obtained with

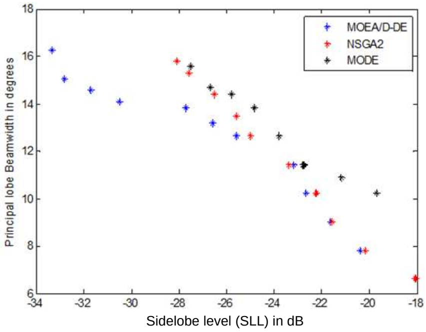

Figure 7. Trade-off curves obtained with three MO algorithm (Case 2).

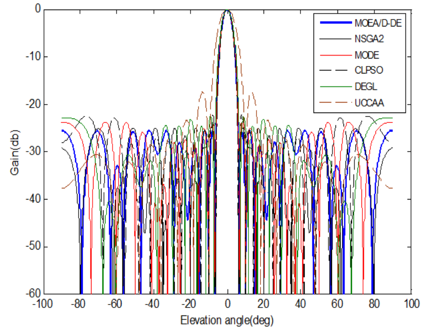

Figure 8. Array pattern for $N_1 = 4$ and $M = 7$.

Table 6. Best, worst, mean, and standard deviations of the performance metrics for comparing the MO algorithms (Case 2).

Performance Metric	Value type	MOEA/D-DE	NSGA-2	MODE
R-indicator	Best	$5.7e-08$	$2.9e-06$	$7.7e-06$
	Worst	$2.5e-05$	$7.1e-04$	$3.8e-03$
	Mean	$5.9e-06$	$6.5e-05$	$2.8e-04$
	Std. Dev.	$1.3e-06$	$7.4e-05$	$3.6e-04$
Hypervolume-indicator	Best	$2.5e-06$	$2.0e-05$	$8.8e-06$
	Worst	$7.2e-05$	$5.9e-04$	$9.1e-04$
	Mean	$1.1e-05$	$2.8e-05$	$3.5e-04$
	Std. Dev.	$8.7e-06$	$4.7e-05$	$9.5e-05$

Table 7. Design objectives achieved.

Objectives	MOEA/D-DE	DEGL	CLPSO	NSGA2	MODE	UCCAA
BW (Degrees)	12.64	13.84	12.67	12.70	12.70	19.68
SLL	-25.58	-22.70	-22.49	-25.06	-23.81	-17.51

single-objective optimization algorithms: CLPSO and DEGL. Mean values of the design objectives are given in Table 7. The experimental results indicate that MOEA/D-DE achieves best design objectives for the second instance as well.

6. COMPARATIVE STUDY WITH NON-UNIFORM EXCITATION

Many recent works in the field of CCAAs have been based on non-uniform excitation method (elements of the same ring being non-uniformly excited). We compare the results obtained with non-uniform excitation method against our proposed method (where excitation across different rings is non-uniform but for elements in the same ring, it is uniform). For both the methods the same algorithm, i.e., MOEA/D-DE is used. Due to space restriction we have showed the results corresponding to the best compromise solution only for a single case corresponding to $N_1 = 4$ and $M = 7$. This is Case 2 in Section 5. For non-uniform excitation method, the 3D pattern is not symmetric. Hence we would need to consider the entire 3D pattern to find the principal lobe BW in solid angles and the SLL.

The 3D plot in the u-v plane is given in Figure 10 and the XZ view of the same is shown in Figure 9. From the results given in

Table 8. Design objectives achieved.

Objectives	Non-uniform ring excitation and non-uniform spacing	Non-uniform excitation
Beamwidth (Steradians)	0.038	0.177
SLL (dB)	-25.58	-18.36

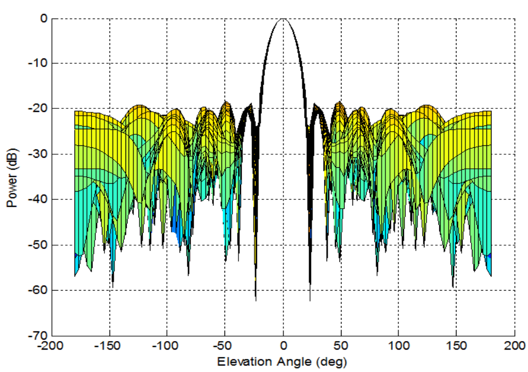

Figure 9. XZ View of 3D pattern.

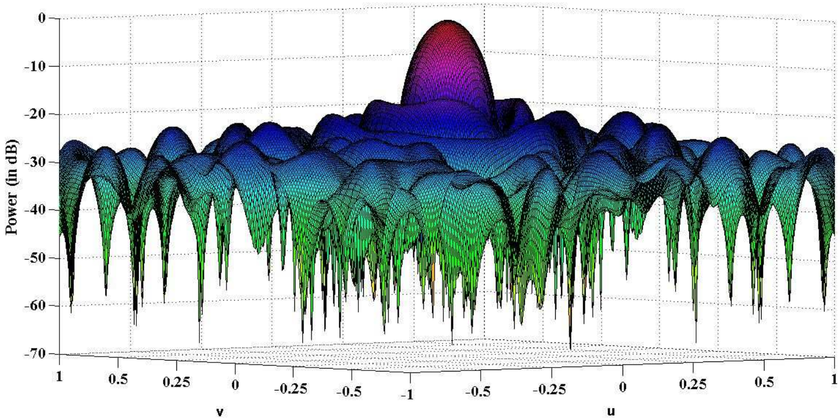

Figure 10. 3D plot for non-uniform excitation method.

Table 8 we see that the non uniform excitation method performed in an inferior manner as compared to our proposed method. Moreover with non-uniform excitation method the design complexity is huge.

7. CONCLUSIONS

We proposed a new multi-objective optimization framework for the design of CCAAs with non-uniform radial spacing and non-uniform excitation across different rings. We optimize the element excitations such that the SLL and BW are simultaneously minimized till an optimal trade-off is reached. Previous works considered a weighted sum approach to handle the two objectives, but the conflicting nature of the objectives (as is evident from the shape of the approximated PFs) makes it necessary to adopt an MO approach. If a weighted sum approach were used we would get only one solution corresponding to a single point on the Pareto Front, which again may not be the best trade-off solution. Location of this solution on the actual PF is in general very much sensitive to the choice of the weights for the two objectives. If the objective that is easier to optimize for a particular algorithm is given larger weight then the other objective will not be sufficiently minimized. However in an MO approach, the objectives are minimized with a view to attaining the best compromise between them. MO algorithms give us a set of Pareto-optimal solutions and this in turn allows greater freedom to the antenna designer to choose a solution that best fits to his design requirement.

An antenna designer needs to satisfy certain design criteria in a cost-effective way. He also needs to fix the number of elements in the first ring and the number of rings in the CCAA. Having fixed those parameters he needs to determine the element excitations such that his design requirements are satisfied. In this article we provided a parametric study, aided by MOEAs, to show how the best compromise solutions depend on N_1 and M. We illustrated how the solutions improve with increase in N_1 and M. We believe that this parametric study will provide a valuable insight to the designer of CCAAs.

We undertook simulations on the CCAA design instances with a very powerful MOEA called MOEA/D-DE. We illustrated that the best compromise solution returned by MOEA/D-DE is able to comfortably outperform the best results obtained with well-known MOEAs like MODE and NSGA-2 as well as state-of the-art single-objective optimization algorithms: DEGL and CLPSO over two significant design instances. Our research indicates that powerful MOEAs can be applied to obtain better results over many problems in electromagnetics, where there are two or more conflicting design objectives that are to be achieved simultaneously. A few examples of such problems are Ultra wideband TEM horn antenna design, wire antenna geometry design, thinned planar circular arrays, radio network optimization etc..

REFERENCES

1. Stearns, C. and A. Stewart, "An investigation of concentric ring antennas with low sidelobes," *IEEE Trans. Antennas Propag.*, Vol. 13, No. 6, 856–863, Nov. 1965.
2. Das, R., "Concentric ring array," *IEEE Trans. Antennas Propag.*, Vol. 14, No. 3, 398–400, May 1966.
3. Dessouky, M. I., H. A. Sharshar, and Y. A. Albagory, "Optimum normalized-Gaussian tapering window for side lobe reduction in uniform concentric circular arrays," *Progress In Electromagnetics Research*, Vol. 69, 35–46, 2007.
4. Bogdan, L. and C. Comsa, "Analysis of circular arrays as smart antennas for cellular networks," *Proc. IEEE Int. Symp. Signals, Circuits and Systems' 03*, Vol. 2, 525–528, Jul. 2003.
5. Roy, G. G., S. Das, P. Chakraborty, and P. N. Suganthan, "Design of non-uniform circular antenna arrays using a modified invasive weed optimization algorithm", *IEEE Trans. Antennas Propag.*, Vol. 59, No. 1, 110–118, Jan. 2011.
6. Chen, T. B., Y. L. Dong, Y. C. Jiao, and F. S. Zhang, "Synthesis of circular antenna array using crossed particle swarm optimization

algorithm," *Journal of Electromagnetic Waves and Applications*, Vol. 20, No. 13, 1785–1795, 2006.

7. Dessouky, M. I., H. A. Sharshar, and Y. A. Albagory, "Efficient sidelobe reduction technique for small-sized concentric circular arrays," *Progress in Electromagnetics Research*, Vol. 65, 187–200, 2006.
8. Dessouky, M., H. Sharshar, and Y. Albagory, "A novel tapered beam forming window for uniform concentric circular arrays," *Journal of Electromagnetic Waves and Applications*, Vol. 20, No. 14, 2077–2089, 2006.
9. Li, Y. and K. C. Ho, "3-D array pattern synthesis with frequency invariant property for concentric ring array," *IEEE Transactions on Signal Processing*, Vol. 54, No. 2, 780–784, Feb. 2006.
10. Kennedy, J. and R. Eberhart, "Particle swarm optimization," *Proc. IEEE Int. Conf. Neur. Net.*, 1942–1948, 1995.
11. Mandal, D., S. P. Ghoshal, and A. K. Bhattacharjee, "Radiation pattern optimization for concentric circular antenna array with central element feeding using craziness-based particle swarm optimization," *International Journal of RF and Microwave Computer-Aided Engineering*, Vol. 20, No. 5, 577–586, Sep. 2010.
12. Mandal, D., S. P. Ghoshal, and A. K. Bhattacharjee, "Optimal design of concentric circular antenna array using particle swarm optimization with constriction factor approach," *International Journal of Computer Applications*, Vol. 1, No. 17, 112–116, 2010.
13. Pathak, N., G. K. Mahanti, S. K. Singh, J. K. Mishra, and A. Chakraborty, "Synthesis of thinned planar circular array antennas using modified particle swarm optimization," *Progress In Electromagnetics Research Letters*, Vol. 12, 87–97, 2009.
14. Li, H. and Q. Zhang, "Multiobjective optimization problems with complicated pareto sets, MOEA/D and NSGA-II," *IEEE Trans. on Evolutionary Computation*, Vol. 12, No. 2, 284–302, 2009.
15. Zhang, Q., W. Liu, and H. Li, "The performance of a new MOEA/D on CEC09 MOP test instances," *Proceedings of the Eleventh Conference on Congress on Evolutionary Computation*, 203–208, 2009.
16. Zhang, Q., A. Zhou, S. Z. Zhao, P. N. Suganthan W. Liu, and S. Tiwari, "Multiobjective optimization test instances for the CEC 2009 special session and competition," Technical Report CES-887, University of Essex and Nanyang Technological University, 2008.
17. Storn, R. and K. Price, "Differential evolution — A simple and efficient heuristic for global optimization over continuous spaces,"

Journal of Global Optimization, Vol. 11, No. 4, 341–359, 1997.
18. Price, K., R. Storn, and J. Lampinen, *Differential Evolution — A Practical Approach to Global Optimization*, Springer, Berlin, 2005.
19. Panduroa, M. A., D. H. Covarrubiasa, C. A. Brizuelaa, and F. R. Maranteb, "A multi-objective approach in the linear antenna array design," *Int. J. Electron. Commun. (AEÜ)*, Vol. 59, 205–212, 2005.
20. Pal, S., B. Qu, S. Das, and P. N. Suganthan, "Optimal synthesis of linear antenna arrays with multi-objective differential evolution", *Progress In Electromagnetics Research*, Vol. 21, 87–111, 2010.
21. Pal, S., S. Das, and A. Basak, "Design of time modulated linear arrays with a multi-objective optimization approach," *Progress In Electromagnetics Research*, Vol. 23, 83–107, 2010.
22. Pal, S., S. Das, A. Basak, and P. N. Suganthan, "Synthesis of difference patterns for monopulse antennas with optimal combination of array-size and number of subarrays — A multi-objective optimization approach," *Progress In Electromagnetics Research*, Vol. 21, 257–280, 2010.
23. Abido, M. A., "A novel multiobjective evolutionary algorithm for environmental/economic power dispatch," *Electric Power Systems Research*, Vol. 65, 71–81, Elsevier, 2003.
24. Tapia, C. G. and B. A. Murtagh, "Interactive fuzzy programming with preference criteria in multiobjective decision making," *Comput. Oper. Res.*, Vol. 18, 307–316, 1991.
25. Liang, J. J., A. K. Qin, P. N. Suganthan, and S. Baskar, "Comprehensive learning particle swarm optimizer for global optimization of multimodal functions," *IEEE Trans. on Evolutionary Computation*, Vol. 10, No. 3, 281–295, Jun. 2006.
26. Das, S., A. Abraham, U. K. Chakraborty, and A. Konar, "Differential evolution using a neighborhood based mutation operator," *IEEE Trans. on Evolutionary Computation*, Vol. 13, No. 3, 526–553, Jun. 2009.
27. Deb, K., A. Pratap, S. Agarwal, and T. Meyarivan, "A fast and elitist multiobjective genetic algorithm: NSGA-II," *IEEE Trans. on Evolutionary Computation*, Vol. 6, No. 2, 182–197, 2002.
28. Xue, F., A. C. Sanderson, and R. J. Graves, "Pareto-based multi-objective differential evolution," *Proceedings of the 2003 Congress on Evolutionary Computation (CEC' 2003)*, Vol. 2, 862–869, Canberra, Australia, 2003.
29. Knowles, J., L. Thiele, and E. Zitzler, "A tutorial on the performance assessment of stochastic multiobjective optimizers,"

Computer Engineering and Networks Laboratory, ETH Zurich, Switzerland, Feb. 2006.

30. Coello Coello, C. A., G. B. Lamont, and D. A. Van Veldhuizen, *Evolutionary Algorithms for Solving Multi-objective Problems*, Springer, 2007.
31. Deb, K., *Multi-objective Optimization Using Evolutionary Algorithms*, John Wiley & Sons, 2001.
32. Zhang, Q. and H. Li, "MOEA/D: A multi-objective evolutionary algorithm based on decomposition," *IEEE Trans. on Evolutionary Computation*, Vol. 11, No. 6, 712–731, 2007.
33. Miettinen, K., *Nonlinear Multiobjective Optimization,* Kuluwer Academic Publishers, 1999.
34. Yang, S., Y. B. Gan, and A. Qing, "Antenna-array pattern nulling using a differential evolution algorithm," *International Journal of RF and Microwave Computer-Aided Engineering*, Vol. 14, No. 1, 57–63, Jan. 2004.
35. Wu, H., J. Geng, R. Jin, J. Qiu, W. Liu, J. Chen, and S. Liu, "An improved comprehensive learning particle swarm optimization and its application to the semiautomatic design of antennas," *IEEE Trans. Antennas Propag.*, Vol. 57, No. 9, 3018–3028, Oct. 2009.
36. Massa, A., M. Pastorino, and A. Randazzo, "Optimization of the directivity of a monopulse antenna with a subarray weighting by a hybrid differential evolution method," *IEEE Antennas and Wireless Propagation Letters*, Vol. 5, 155–158, 2006.
37. Haupt, R. L., "Optimized element spacing for low sidelobe concentric ring arrays," *IEEE Trans. Antennas Propag.*, Vol. 56, No. 1, 266–268, 2008.